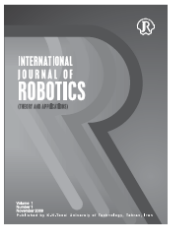

INTERNATIONAL JOURNAL OF ROBOTICS
(THEORY AND APPLICATIONS)
E-mail: IJR@kntu.ac.ir

The Complete Design of Lower Limb Extremity Exoskeleton Robot with Capability of Extending a Control Approach to Semi-Active Mode by Hardware in the Loop Method

M. Ahmadi Kermanshahi[a], F. Cheraghpour Samavati[b*] and A. Ghaffari[c,]

[a] Department of Mechanical Engineering, Islamic Azad University Tehran South Branch, Tehran, Iran, P.O. Box, 19977-53951
[b] Department of Mechanical Engineering, Islamic Azad University Pard. C., Tehran, Iran,
[c] Faculty of Mechanical Engineering, K. N. Toosi University of Technology, Tehran, Iran, P.O. Box, 19395-1999

ARTICLE INFO

Article history:
Submit: 2025-06-02
Revise: 2025-10-13
Accept: 2025-11-08

Keywords:
Exoskeleton
Rehabilitation
Dynamic Modeling
Hardware in the Loop

ABSTRACT

In this paper, a lower limb extremity exoskeleton robot is presented to support people with disabilities in the walking process and rehabilitation. The first section presents the conceptual design of the robot model, which indicates that the robot has seven degrees of freedom. Then the dynamic model of the mechanical system of the exoskeleton has been shown. In order to dynamic simulation, the mechanical model is transferred from the CATIA to MATLAB and simulated in SimMechanics, by applying the system parameters and implementing a complete process of gait cycle. In the following, a combinative controller is designed based on the described system. Finally, the gained results planted on the prototype of the presented system and the given parameters are tested in a loop by placing the control system hardware in a real-time situation. And the results of this approach demonstrated a good response from the control hardware output of the learning system for the semi-active mode in the exoskeleton.

1. Introduction

Improving quality of life is a goal of modern society. Quality of life studies assess the physical condition [1]. Population aging is one of the pressing global issues that can affect the quality of life, so it should demand an immediate response by implementing policies and programs to support the elderly and their families [2]. There are many factors that reduce the functional capacity, including both ability and intensity, for movement tasks such as level walking or climbing stairs [2]. Robotic systems are purposed as one of the solutions for the issues that can assist healthcare providers in various tasks, such as medication administration, patient monitoring, and rehabilitation [3]. The rehabilitation robots are directly serving humans and have extensive

* Corresponding address: Department of Mechanical Engineering, Islamic Azad University, Pardis Branch, Tehran, Iran,
Tel.: +98 2176281010;
E-mail address: farzad.samavati@iau.ac.ir.

application prospects in rehabilitation therapy with high professional requirements [4]. Therefore, it is of great importance to develop advanced rehabilitation robots [5], [6]. Considering that these robots interact with humans in the applications of these types of systems, it should be noted that the robot must be capable of executing high-precision, error-free commands, as the robot generally must repeat the behavior patterns of the rehabilitation specialist with high accuracy [7]. In this paper we focus on one kind of rehabilitation robot which is called an exoskeleton. The exoskeleton is a wearable mechanical device worn in parallel with the human body and has become more commonplace in recent years [8], [9]. It is also known as a wearable robotic system which can be worn to help human beings to support and protect parts of their bodies [10]. It can also be described as helping people to achieve the highest level of performance, independence, and quality of possible life [11]. Exoskeleton robots include interdisciplinary topics including biomechanics, robotics, synthetic and biosensor technology, and control engineering [12]. Exoskeletons can increase user endurance, strength, and/or functionality of human movement. With this goal in mind, engineers have developed robotic exoskeletons that can aid healthy human users by reducing the muscle activation and muscle work required to perform some tasks [13], [14]. In many industries, exoskeletons have been used to increase worker strength [15]. Therefore, studies have shown exoskeletons as a potential intervention to reduce physical demands [16]. The application of the exoskeleton to the human body can be divided into three locations: (1) throughout the human body [17], (2) at the upper part of the human body, such as the torso and arms [18], and (3) at the lower part of the human body, i.e., from the waist down [19]. They also divided into active and passive general categories. For the upper body limb, the impact of a passive back-support exoskeleton on muscle activity and kinematics in a repetitive lifting and carrying task in a study showed that the exoskeleton decreased trunk muscle activity (3-7 percent), and the kinematic parameters also exhibited improvements, specifically in terms of the peak flexion angles [20], [21]. The lower limbs of the human body have more important roles than the other parts. This is because lower limbs generate more torque than other parts while walking [22]. So that for lower limb movement disorders, active rehabilitation training should be started as early as possible [23]. Although great progress has been made in the century-long effort to design and implement robotic exoskeletons, there are still many challenges. Many factors still continue to restrain the performance of exoskeletons; for example, the transition of the operation status can lead to a discontinuous system dynamic, making it challenging to achieve a stable, continuous, and accurate torque tracking [24]. A significant challenge is how to effectively control the exoskeletons to bring their performance into full play [25]. Because research has shown that the active exoskeleton improves the work performance aspect of users' functional performance more compared to the passive exoskeleton [26]. Therefore, control strategy is one of the most important issues [27]. In order to tackle the exoskeleton control problem, several approaches have been proposed, e.g., sensitivity amplification [28], predefined gait trajectory control [28], [29], model-based control [30], [31], adaptive control [32], fuzzy control [33], [34], and sliding mode control [35]. These control strategies are used for different exoskeletons, and each has its own advantages and disadvantages. Particularly, some control strategies require an exact model. Nevertheless, obtaining an accurate model is difficult in practice, since too many kinematic and dynamic variables are required to be recognized by utilizing diverse sensors. Furthermore, the control strategy should reduce the influence from external disturbances to ensure the stability of the system [36]. Wearable exoskeletons have attracted more research interests due to their wide range of applications, such as relieving the heavy rehabilitation work, helping paraplegic or quadriplegic people regain locomotion, empowering healthy people to carry heavy loads, and providing additional power for walking [37]. In this paper the steps of manufacturing of a lower limb exoskeleton has been shown which is designed to aid people for walking. Several control approaches are applied to reach the best procedure among them.

2. Conceptual Design

The main purpose in the design of this robot is to achieve an integrated mechanism that connects to the lower extremity and performs joint behavior with its own intelligence so that the disabled person can experience the walking process independently. The torque of each joint is supplied by electro-motors that provide the rate of opening and closing of the links of each joint at each stage of the process. Therefore, the most important sensor associated with robot mechanics is the shaft encoder. Shaft encoders are placed on the shaft of each joint; therefore, the amount of change in the angle of each joint can be checked and the instructions required. Hydraulic and pneumatic jacks are high power, but in some cases electric motors are used to reduce energy consumption during the step process [38]. Figure 1 shows our mechanical hardware of the

exoskeleton robot with a passive wheel walker aid to keep user stable.

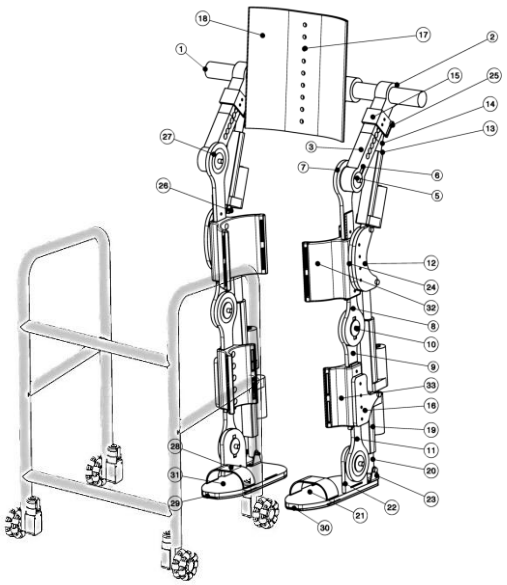

Figure 1. Mechanical hardware of Exoskeleton robot, designed and simulated in CATIA.

Then all components were designed based on the position and stresses. After structural modeling in CATIA software and completing the technical drawings, the stress analysis was performed according to the user's anatomy, so the model under study is capable of serving people with a height range of 170-190 cm and a weight range of 60-90 kg during the operation, and the reliability coefficient was calculated for all under-stress components that are forming the robot platform. Figure 2 illustrates the contour for the foot piece tension and the joint shaft.

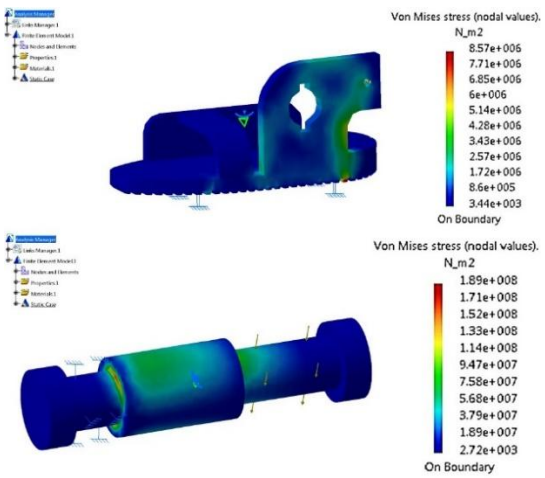

Figure 2. Stress analysis of the foot related part and the connector shaft on Van-Mises criterion.

3. Dynamic Modeling

The human gait cycle consists of two phases: swing and stance. The walking cycle begins with the start of the stance phase (foot on the ground) at heel-strike, followed by toe-off and the swing phase (foot off the ground) beginning at around 60% of the cycle [10]. Dynamic equations of motion for a foot with three joints and three links can be achieved by directly applying Newton's laws of motion by considering the final member as a joint connected to the ground and eliminating part of the step process that is actually a step in with both feet on the ground. Newton's equations are relatively complicated to obtain. The Lagrange method is used in this paper.

Firstly, kinetic energy and potential energy terms are calculated for each link, assuming that their movements do not leave the page.

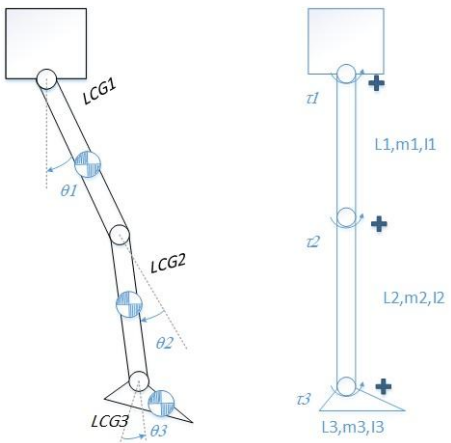

Figure 3. description of generalized coordinates in the leg model.

Kinetic energy for the first link (thigh) is coming below:

$$T_1 = \frac{1}{2}\left[m_1\left(l_{CG1}\dot{\theta}_1\right)^2 + I_{CG1}\left(\dot{\theta}_1\right)^2\right] \quad (1)$$

Second link (shank) kinetic energy equation is:

$$T_2 = \frac{1}{2}m_2[\left(l_1\dot{\theta}_1\right)^2 + \left(l_{CG2}\left(\dot{\theta}_1 + \dot{\theta}_2\right)\right)^2 + 2l_1 l_{CG2}\dot{\theta}_1\left(\dot{\theta}_1 + \dot{\theta}_2\right)\cos\theta_2] + \frac{1}{2}I_2\left(\dot{\theta}_1 + \dot{\theta}_2\right)^2 \quad (2)$$

And the third link (foot) is:

$$T_3 = \left(\frac{1}{2}m_3\left(l_1\dot{\theta}_1\right)^2\right) + \frac{1}{2}m_3\left(l_2\left(\dot{\theta}_1 + \dot{\theta}_2\right)\right) + \frac{1}{2}m_3\left(l_{CG3}\left(\dot{\theta}_1 + \dot{\theta}_2 + \dot{\theta}_3\right)\right)^2 + m_3 l_1 l_2 \dot{\theta}_1\left(\dot{\theta}_1 + \dot{\theta}_2\right)\cos\theta_2{}^2 + \frac{1}{2}m_3 l_1 l_3 \dot{\theta}_1\left(\dot{\theta}_1 + \dot{\theta}_2 + \dot{\theta}_3\right)\cos(\theta_1 + \theta_2) + \frac{1}{2}m_3 l_2 l_3\left(\dot{\theta}_1 + \dot{\theta}_2\right)\left(\dot{\theta}_1 + \dot{\theta}_2 + \dot{\theta}_3\right) + \frac{1}{2}I_3\left(\dot{\theta}_1 + \dot{\theta}_2 + \dot{\theta}_3\right)^2 \quad (3)$$

Now the potential energy of links shown in 8 to 10 equations respectively:

$$U_1 = m_3 g l_{CG3} \cos(\theta_1 + \theta_2 + \theta_3) + \frac{1}{2} k_3 \theta_3^2 \quad (4)$$

$$U_2 = m_2 g l_3 \cos(\theta_1 + \theta_2 + \theta_3) + m_2 g l_{CG2} \cos(\theta_1 + \theta_2) + \frac{1}{2} k_2 \theta_2^2 \quad (5)$$

$$U_3 = m_1 g l_3 \cos(\theta_1 + \theta_2 + \theta_3) + m_1 g l_2 \cos(\theta_1 + \theta_2) + m_1 g l_{CG1} \cos(\theta_1) + \frac{1}{2} k_1 \theta_1^2 \quad (6)$$

Then the general equations for one leg shown as follows.

$$\boldsymbol{M(\theta)\ddot{\theta} + C(\theta + \dot{\theta})\dot{\theta} + P(\theta) = Q} \quad (7)$$

In which $M(\theta)$ is a 3×3 matrix of inertia which is a function of angle. $C(\theta + \dot{\theta})$ is a 3×3 centripetal and Coriolis forces matrix. $P(\theta)$ is a gravity torque vector is a 3×1 matrix. Finally, Q which we describe it as generalized forces, refers to the external forces applied to the system. These forces are the torque generated by the actuators mounted on each joint, which is applied as a 3×1 vector, and the operation of these actuators is related to the joint angle at any given moment. also, the force exerted by the pilot on the robot as well as the surface reaction are applied in the form of other vectors in this generalized force that are not currently discussed and will be presented in later work. For the equation related to the motion of the other leg, there is an equation with the same feature that will be generated. The only difference between the two equations is the difference in the angles of the same joints [39].

To simulate the mentioned equations in SimMechanics space (or meclib) in MATLAB, some factors are needed. So, by using the material properties and geometrical parameters of the CATIA model of the robot, the values of the moment of inertia matrix of each link are obtained. Also, values were applied in dynamic simulation for a user with a height of 179 cm and a weight of 80 kg. In the present approach, the dynamic features of the robot and the user's limb are considered in the model at the same time, so the studied system is the lower limb of the user with the robot. As a result, inertia matrices for the thigh, shank, and foot are calculated at this stage. Which are indicated in table 1.

Table 1. inertia momentum of each extremity

Links	$I_{xx}[kg\times m^2]\times10^{-3}$	I_{yy}	I_{zz}
Thigh	73	66	15
Shank	66	60	11
foot	13	11	4

By considering the mentioned coordinate as the coordinate reference system (CRS), the center of masses for each member will be reachable. Center of mass is shown in table 2. Also, we should know that the positions below are related to the CRS, and they have been validated with CATIA.

Table 2. Center of masses of each extremity

Links	$x_{CG}[m]\times10^{-3}$	y_{CG}	z_{CG}
Thigh	298	-106	-241
Shank	222	-573	-329
foot	360	-957	-141

According to the data we have, we will produce a dynamic model in the toolbox of MATLAB software. This system consists of 7 members that are connected by 6 joints. The entire upper body is named as “trunk” in the model. The following figure shows the knees model, which contains the knee patella condition in the software, according to the ordinary name of members.

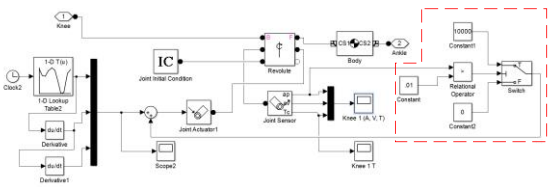

Figure 4. the knee patella for dynamic model of robot in SimMechanics space.

4. Controller Design

Since the nature of the system under study is defined as a tool for rehabilitation, it must be able to interact with a variety of lower limb disabilities. Therefore, in the process of the combined control system, two methods have been used to fulfill this task. A schematic of the control system is given in Figure 5.

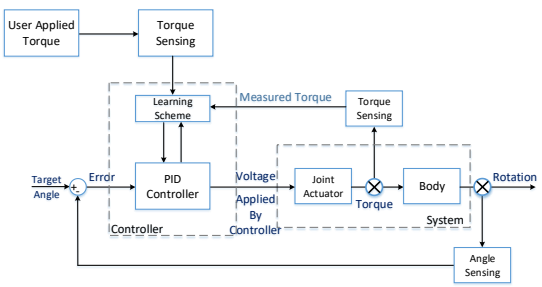

Figure 5. The robot interaction with the pilot in presence of a combined control system.

At the beginning of the explanation of the figure, it should be noted that rehabilitation equipment will accustom the muscles to perform the correct pattern related to a specific behavior by repeatedly repeating a behavior in a defective limb [40]. Therefore, the robot must be able to be used both for people with complete disabilities and for people who have lost part of their limb’s ability.

For the first case, when the user has completely lost the ability of his lower limb, it is so that because all the torque required by the joints will be provided by the actuators, we will only need to control the position of the actuators with the shaft encoders, which are built-in for the robot, and using their feedback by a PID controller, it will be done. But for another capability of this robot, when part of the torque required by the gait cycle is provided by the person himself, in other words, the user has not lost all the power of his lower limb, the importance of one part of the model shown in Figure 5 as a learning system will appear in the controller. Thus, the maximum torque that a person needed is entered into the learning system, and the applied torque is obtained by load cells that are installed in each part of the exoskeleton. Then, the PID controller, by playing its role and controlling the position of the joint, applies torque to the joint, the amount of which will be re-examined by the learning system.

The system generates a torque pattern from the combination of the two feedbacks and transmits it to the controller, which prevents the actuator from applying additional force by considering a target function that depends on the pilot power intensity. According to the recent explanation for the learning system, we will need a function estimator to combine the two input functions and obtain the objective function. To achieve this, two types of artificial neural networks have been used, which are radial basis networks and multi-layer perceptrons. In this section, the MLP and RBF artificial neural networks designed for the hip joint are introduced, and their results are announced in figure 6 and figure 7. In order to estimate the force function on the hip joint, the results of the previous sections were used. This MLP network consists of three neurons in the middle layer, two neurons in the input layer, and one neuron in the output layer. For the RBF, it should say, this network has a maximum of 10 neurons. The neurons of the force input are estimated by the user with 80% of the body power and also the second input of the force applied to the joint by the hip operator. Therefore, we have:

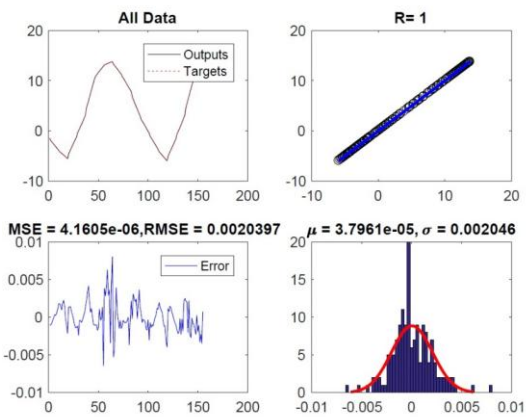

Figure 6. The MLP Neural Network results

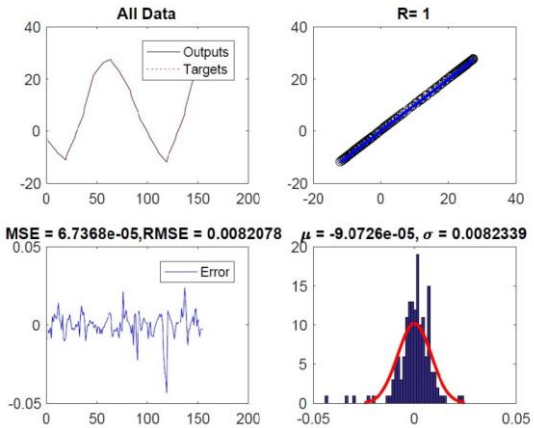

Figure 7. The RBF Neural Network results

In order to check Figure 6 & 7, it is necessary to mention some points. At first, we will introduce the four available charts in each figure, and then we will check their results. The upper left diagram shows the adaptation of the network output data to the target data, which can be said to match each other with a good approximation. The upper right graph shows the correlation coefficient of the objective function and the output of the network, which has reached its maximum value of 1. The lower left diagram shows the amount of network error in the entire training process, which is very small, and the network tries to make this amount as low as possible. Also, in this graph, the mean square error (MSE) and its square root (RMSE) are also calculated and shown. And the final diagram is the error dispersion, which shows the level of reliability of the network. It also shows the standard deviation diagram, which obviously, the lower the bandwidth, the higher the accuracy of the network. The average error and standard deviation values are shown numerically.

So that the controller is useful for the system in several ways. First, people who have lost part of their power in their limbs suffer from muscle tremors during their activities. And the artificial network, by choosing the right weights for inputs, can remove the vibrations. Therefore, the output of the joint operator does not have extra noises. The second advantage is that the patterns in the control system must change robustly because of its usage for rehabilitation. So that if, due to tiredness or nervous shocks, a sudden force from the pilot to the system causes the controller to not react quickly, or the necessary power is not supplied. Unless the functional pattern changes for the system repeatedly, so that the network can train with the new pattern and adjust the command settings again to a new pattern. This causes the pilot to be forced to apply the appropriate force, and if the power increases, it will not return to the previous state. It

will also increase the user range of this robot. Thus, for disabilities with different intensities, it is enough to go through the training steps according to the pilot's ability in the robot to achieve the robot settings in a suitable state with the pilot. In the following, we will investigate the diagrams obtained from the simulation of the above items on the hip joint and thigh as a sample in MATLAB software.

The diagram of changes in hip torque during the gait cycle is also shown in Figure 8.

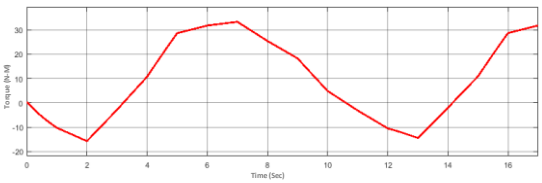

Figure 8. Torque changes required by the hip joint for the gait process.

The figure shows a state of operation in which the user does not apply any force; in other words, the user has a complete disability for the thigh muscle. In the following, we will investigate the situation in which the user will be able to provide part of the required force to the hip joint; thus, the torque pattern is entered into the system in a noisy form for a person whose thigh muscle is 20% capable, and it is shown in Figure 9, which is the torque produced by the operator.

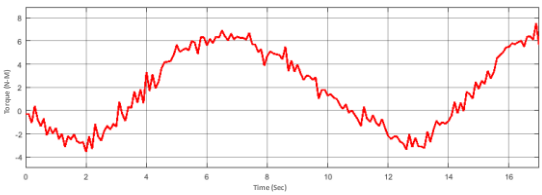

Figure 9. user input torque on the hip for semi-active mode.

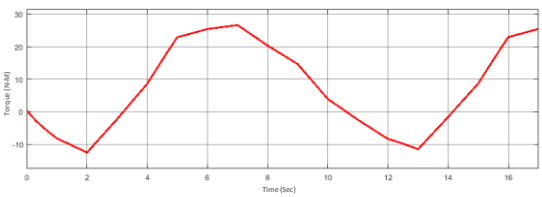

Figure 10. Input torque from hip joint actuator in semi-active mode.

According to figure 10, the output torque of the actuator does not consist of any noise, which is an advantage for the combined controller.

Then it must be ensured that this simulation process can be implemented practically. Therefore, the steps are performed according to Figure 11, known as the “V” Diagram, which is used to model-based designed systems. This is a generalized and abstract rendition of the “V” process that is familiar to automotive engineers.

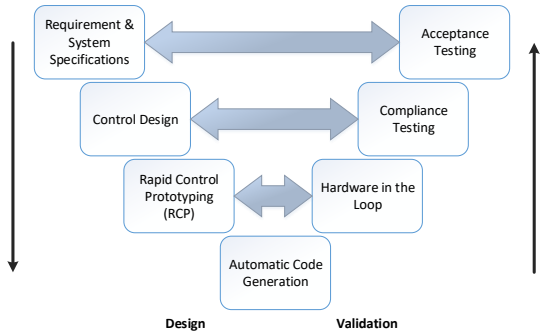

Figure 11. V-Diagram for Model Based System Design.

The V-Diagram model is a development process model that can be viewed as an extension of the waterfall model. Instead of moving down linearly, the process steps are redirected upward after the coding phase to form the typical V shape like Figure 12. The V-Diagram model demonstrates the relationships between each phase of the development life cycle and its associated phase of testing [41].

First, the output of the Simulink model must be executed in real-time, not when the program is set by default. For this purpose, the real-time Windows target is used. In this approach, the operating system time (Windows) will be available and will not be determined by the computer processor (CPU) clock. Next, with the help of the ability to auto-code generate in MATLAB software, we convert the Simulink model into a "C" programming language code. The Simulink space is initially set as a variable step. In this way, it considers the integration steps in proportion to the speed of the function change rates. However, in order to perform the desired operation, the integral steps must always be set in a fixed step. Where the appropriate solution method must be selected. Since in dynamic systems, the more severe the system changes, the more integral error there will be, and there are no such changes in this robot, the Runge-Kutta rank 4 method gives us proper results. It should be mentioned that in this prototype, an ARDUINO 2560 processor has been used as the main processing core of the robot.

After these steps, the system processor is placed in a loop with the computer in which the system is dynamically modeled, with the difference that this time the controller is not present in Simulink, and instead the processor receives the model outputs via serial cable and the appropriate control command. Sends to the model again via serial connection. This step is inevitable to validate the performance of the control system on the processor. So that it would be expressible that the controller is reasonably successful in performing its tasks in the loop.

Using Simulink for the processor requires receiving an Arduino toolbox in the Simulink environment to be able to use its inputs and outputs.

It also transmitted data as code through data transfer bases to its CPU and received the necessary outputs from it. In serial data transfer, the volume of data must always be reduced. This is because the time interval for each transfer period is reduced, and the operating frequency of the system can be considered less to reduce system noise. Therefore, the data must be sent as packet data. To be able to manage data transfer from different sensors through one port. Since each sensor can send two bytes of data, which transmit six bytes of data per foot at a time, and to prevent errors in receiving data, two bytes are identified as a header for each packet. Also, to avoid the system error, two bytes are provided to sum all data bytes, which are called Check Sum, so the sent data packets contain 10 bytes.

5. Conclusions

After the above steps, the motion animation was run, and the robot's walking cycle was reviewed. All the links that make up the system were entered in the software, and then the result was presented in animation mode in Figure 12.

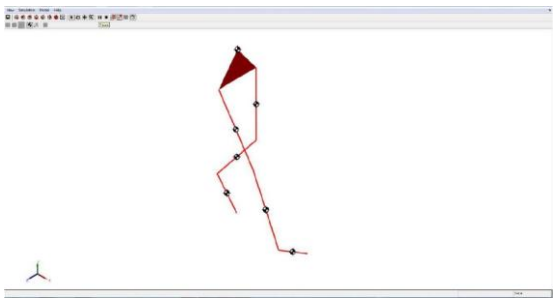

Figure 12. Image of animation model running commands.

Then the correctness of the results was checked with the help of other outputs, such as determination of error on system response, which is shown in Figure 13.

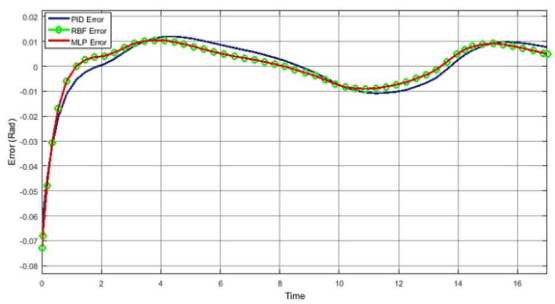

Figure 13. system error in presence of combined controller for right thigh.

According to Figure 13, the initial error of the PID mode is less than that of the integrated controller, but in the continuation of the process, the integrated controller shows better performance, and its steady-state error is less than that of the PID controller. As a result, the integration process of the controller has had a positive effect on the system's performance. In the following, to verify the models and compare the results, we will examine the torques for the hip joint in a state other than the previous state. For this purpose, the diagram in Figure 14 is extracted, in which the torque applied by the user to the robot is shown in purple. Also, the total torque required for the hip joint in the gait cycle is shown in red. Other diagrams are the remaining torques, which are applied by the control system to supply all the needed torque in the whole cycle, which the pilot is unable to apply.

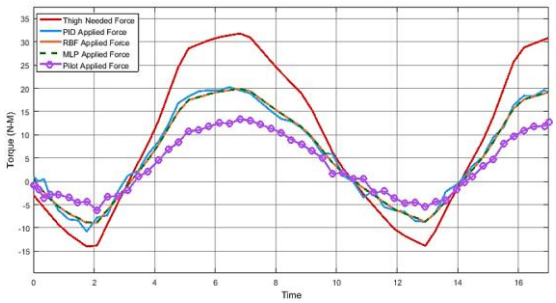

Figure 14. Comparison of torques entered the system and their reactions.

In this case, the user is only able to apply 40% of the required torque, which is accompanied by vibrations due to medical considerations. According to the diagrams in Figure 14, it can be said that the behavior of the system with the presence of two types of neural networks is almost the same. Also, due to the robust structure of this type of controller, noise behavior is not seen in comparison to the PID controller. There are several advantages. Firstly, it does not cause vibration to the user's body, and secondly, it prevents the depreciation of the actuators, etc. Another thing that can be explained about this diagram is that since this diagram is drawn for the hip joint and for a person with 40% of the limb power in the thigh muscle, it can be said that the result of the robot and user output forces will provide the required force of the joint well. Also, the presence of the combined controller allows adjusting the actuators torque accordingly by constantly repeating the individual behavior so that the controller is going to train by increasing the power of the pilot (if the improvement process is positive), and then the actuators apply less torque to the pilot’s limbs. In this context, the performance of the joint to adapt to the target function should also be examined and compared for different situations.

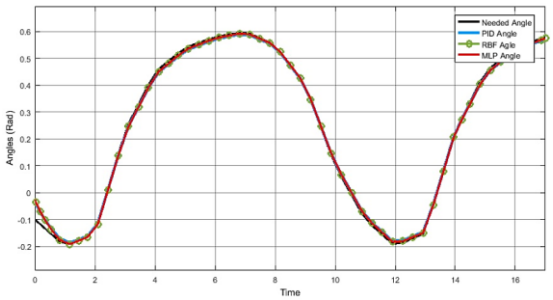

Figure 15. diagram of hip angle change in presence of controllers during the gait cycle.

In Figure 15, it should be noted that our target function diagram is drawn in black. However, due to the very proximity of the controllers' output diagrams to each other, the magnification of the first two seconds of this cycle is shown in Figure 16. This is a comparison of different performance modes of the system for the dynamic model.

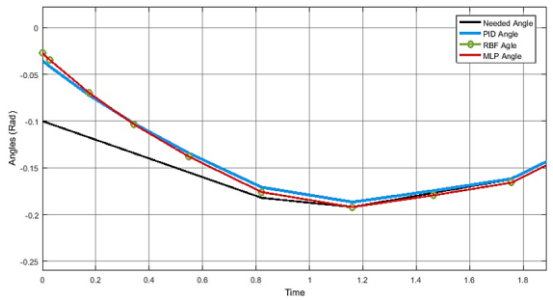

Figure 16. the first two seconds of gait cycle magnification in presence of different control approaches.

In the explanation of figure 16, it should be said that initially the distance from the desired angle for the controllers is large, but then they have a good adaptation to the target function. Also, according to the diagrams, the system response with the integrated controller is closer to the target than the PID controller.

Since all approaches have the capability to be used in every mentioned mode of robot, our focus is on the semi-active. So that we show in active and semi-active modes of the exoskeleton in collaboration with each kind of ANNs system, the response would be more stable and reliable in known and unknown situations. Finally, Figure 17 shows the exoskeleton robot on the pilot's body.

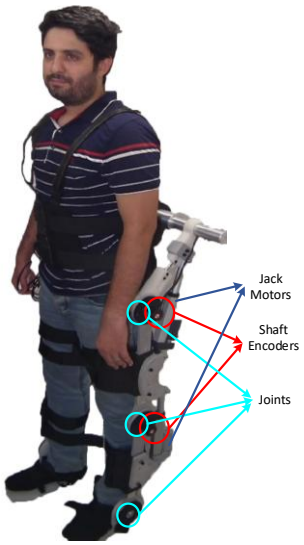

Figure 17. the first two seconds of gait cycle magnification in presence of different control approaches.

6. Reference

[1] Grimmer, M., Riener, R., Walsh, C. J. & Seyfarth, A. Mobility related physical and functional losses due to aging and disease-a motivation for lower limb exoskeletons. Journal of neuroengineering and rehabilitation 16, 1–21 (2019). DOI : 10.1186/s12984-020-0648-z

[2] Jalal, M. F. A., Harith, H. H., Hasan, W. Z. W., Salim, M. S. & Lin, T.-T. Exoskeletons for elderly activity of daily living assistance: A review of upper limb exoskeletons and assessments. International Journal of Integrated Engineering 16, 87–105 (2024). DOI :10.30880/ijie.2024.16.01.008

[3] Ferris, D. P. The exoskeletons are here. Journal of neuroEngineering and rehabilitation 6, 1–3 (2009). DOI: 10.61386/imj.v7i2.422

[4] Siviy, C. et al. Opportunities and challenges in the development of exoskeletons for locomotor assistance. Nature Biomedical Engineering 7, 456–472 (2023). DOI: 10.1186/s10033-019-0389-8

[5] Miao, M. d., Gao, X. s., Zhao, J. & Zhao, P. Rehabilitation robot following motion control algorithm based on human behavior intention. Applied Intelligence 53, 6324–6343 (2023). DOI: 10.1007/s10489-022-03823-7

[6] u, F. et al. The use of sports rehabilitation robotics to assist in the recovery of physical abilities in elderly patients with degenerative diseases: A literature review, Vol. 11, 326 (MDPI, 2023). DOI: 10.3390/healthcare11030326.

[7] Malcolm, P., Derave, W., Galle, S. & De Clercq, D. A simple exoskeleton that assists plantarflexion can reduce the metabolic cost of human walking.

PloS one 8, e56137 (2013). DOI: 10.3233/thc-2011-0646

[8] Dollar, A. M. & Herr, H. Lower extremity exoskeletons and active orthoses: Challenges and state-of-the-art. IEEE Transactions on robotics 24, 144–158 (2008). DOI: 10.1186/1743-0003-6-17

[9] Verville, R. War, politics, and philanthropy: the history of rehabilitation medicine (University Press of America, 2009). DOI: 10.1038/s41551-022-00984-1

[10] Galle, S., Malcolm, P., Collins, S. H. & De Clercq, D. Reducing the metabolic cost of walking with an ankle exoskeleton: interaction between actuation timing and power. Journal of neuroengineering and rehabilitation 14, 1–16 (2017). DOI: 10.1109/tro.2008.915453

[11] Barrutia, W. S., Bratt, J. & Ferris, D. P. A human lower limb mechanical phantom for the testing of knee exoskeletons. IEEE Transactions on Neural Systems and Rehabilitation Engineering (2023). DOI: 10.1353/bhm.2010.a408222

[12] Xu, H., Li, Y., Tang, B. & Xiang, K. The mechanical design and torque control for the ankle exoskeleton during human walking, 26–37 (Springer, 2019). DOI: 10.1007/978-3-030-27541-9_3

[13] Guizzo, E. & Goldstein, H. The rise of the body bots [robotic exoskeletons]. IEEE spectrum 42, 50–56 (2005). DOI: 10.1186/s12984-017-0235-0

[14] Hessinger, M., Pingsmann, M., Perry, J. C., Werthsch¨utzky, R. & Kupnik, M.Hybrid position/force control of an upper-limb exoskeleton for assisted drilling, 1824–1829 (IEEE, 2017). DOI: 10.1109/tnsre.2023.3276424

[15] Christensen, S. et al. Axo-suit-a modular full-body exoskeleton for physical assistance, 443–450 (Springer, 2019). DOI: 10.1371/journal.pone.0056137

[16] So, B. C. L., Hua, C., Chen, T., Gao, Q. & Man, S. S. Biomechanical assessment of a passive back-support exoskeleton during repetitive lifting and carrying: Muscle activity, kinematics, and physical capacity. Journal of safety research 83, 210–222 (2022). DOI: 10.1080/00140139.2023.2240045

[17] Golabchi, A. et al. A framework for evaluation and adoption of industrial exoskeletons. Applied Ergonomics 113, 104103 (2023). DOI: 10.1109/mspec.2005.1515961

[18] Gonzales, A. et al. The compatibility of exoskeletons in perioperative environments and workflows: an analysis of surgical team members' perspectives and workflow simulation. Ergonomics 67, 674–694 (2024). DOI: 10.1109/iros.2017.8205997

[19] Pamungkas, D. S., Caesarendra, W., Soebakti, H., Analia, R. & Susanto, S. Overview: Types of lower limb exoskeletons. Electronics 8, 1283 (2019). DOI: 10.1007/978-3-030-00365-4_52

[20] Shi, D., Zhang, W., Zhang, W. & Ding, X. A review on lower limb rehabilitation xoskeleton robots. Chinese Journal of Mechanical Engineering 32, 1–11 (2019). DOI: 10.1016/j.jsr.2022.08.017

[21] G. . L. R. Global, regional, and country-specific lifetime risks of stroke, 1990 and 2016. New England Journal of Medicine 379, 2429–2437 (2018). DOI: 10.1016/j.apergo.2023.104103

[22] Munih, M. & Bajd, T. Rehabilitation robotics. Technology and Health Care 19, 483–495 (2011). DOI: 10.3390/electronics8111283

[23] Yan, T., Cempini, M., Oddo, C. M. & Vitiello, N. Review of assistive strategies in powered lower-limb orthoses and exoskeletons. Robotics and Autonomous Systems 64, 120–136 (2015). DOI: 10.1056/nejmoa1804492

[24] Young, A. J. & Ferris, D. P. State of the art and future directions for lower limb robotic exoskeletons. IEEE Transactions on Neural Systems and Rehabilitation Engineering 25, 171–182 (2016). DOI: 10.1109/tro.2024.3381556/mm1

[25] Govaerts, R. et al. The impact of an active and passive industrial back exoskeleton on functional performance. Ergonomics 67, 597–618 (2024). DOI: 10.1109/tnsre.2016.2521160

[26] Liao, H. et al. Design, control and validation of a novel cabledriven series elastic actuation system for a flexible and portable back-support exoskeleton. IEEE 11Transactions on Robotics (2024). DOI: 10.1080/00140139.2023.2236817

[27] Chen, C.-F. et al. Active disturbance rejection with fast terminal sliding mode control for a lower limb exoskeleton in swing phase. IEEE Access 7, 72343–72357 (2019). DOI: 10.1109/access.2019.2918721

[28] Kazerooni, H., Racine, J.-L., Huang, L. & Steger, R. On the control of the Berkeley lower extremity exoskeleton (bleex), 4353–4360 (IEEE, 2005). DOI: 10.5772/51903

[29] Sanz-Merodio, D., Cestari, M., Arevalo, J. C. & Garcia, E. Control motion approach of a lower limb orthosis to reduce energy consumption. International journal of advanced robotic systems 9, 232 (2012). DOI: 10.1109/robot.2009.5152394

[30] Kwa, H. K. et al. Development of the ihmc mobility assist exoskeleton, 2556–2562 (IEEE, 2009). DOI: 10.3390/s18030909

[31] Wang, L., Du, Z., Dong, W., Shen, Y. & Zhao, G. Intrinsic sensing and evolving internal model control of compact elastic module for a lower

extremity exoskeleton. Sensors 18, 909 (2018). DOI: 10.1016/s1672-6529(16)60397-9

[32] Long, Y. et al. Development and analysis of an electrically actuated lower extremity assistive exoskeleton. Journal of Bionic Engineering 14, 272–283 (2017). DOI: 10.1016/j.isatra.2013.05.003

[33] Kang, H.-B. & Wang, J.-H. Adaptive control of 5 dof upper-limb exoskeleton robot with improved safety. ISA transactions 52, 844–852 (2013). DOI: 10.1109/tfuzz.2014.2317511

[34] Li, Z., Su, C.-Y., Li, G. & Su, H. Fuzzy approximation-based adaptive back stepping control of an exoskeleton for human upper limbs. IEEE Transactions on Fuzzy Systems 23, 555–566 (2014). DOI: 10.1109/tmech.2006.878550

[35] Kong, K. & Jeon, D. Design and control of an exoskeleton for the elderly and patients. IEEE/ASME Transactions on mechatronics 11, 428–432 (2006). DOI: 10.1155/2016/5017381

[36] Long, Y., Du, Z.-j., Wang, W.-d. & Dong, W. Robust sliding mode control based on ga optimization and cmac compensation for lower limb exoskeleton. Applied bionics and biomechanics 2016, 5017381 (2016). DOI: 10.1109/tfuzz.2014.2317511

[37] Li, Z., Su, C.-Y., Li, G. & Su, H. Fuzzy approximation-based adaptive backstopping control of an exoskeleton for human upper limbs. IEEE Transactions on Fuzzy Systems 23, 555–566 (2014). DOI: 10.1016/j.robot.2014.09.032

[38] Colombo, G., Joerg, M., Schreier, R., Dietz, V. et al. Treadmill training of paraplegic patients using a robotic orthosis. Journal of rehabilitation research and development 37, 693–700 (2000). DOI: 10.1177/154596839901300166

[39] Zoss, A. & Kazerooni, H. Design of an electrically actuated lower extremity exoskeleton. Advanced Robotics 20, 967–988 (2006). DOI: 10.1163/156855306778394030

[40] Taha, Z., Majeed, A., Tze, M. & Rahman, A. G. A. Preliminary investigation on the development of a lower extremity exoskeleton for gait rehabilitation: A clinical consideration. Journal of Medical and Bioengineering Vol 4, 82–85 (2015). DOI: 10.12720/jomb.4.1.1-6

[41] Ulsoy, A. G., Peng, H. & C, akmakci, M. Automotive control systems (Cambridge University Press, 2012). DOI: 10.1017/cbo9780511844577

Biography

Morteza A. Kermanshahi is Master's degree graduate. He received his BSc. In mechanical engineering from Islamic Azad University Qazvin branch, and his MSc. degree in mechanical engineering from Islamic azad university Tehran south branch in 2012 and 2018 respectively. His research interests include dynamic and control of Human-interactive robots and assistive robotic systems.

Farzad Cheraghpour Samavati is currently an assistant professor in the faculty of Mechanical Engineering at Pardis Science & Technology branch of Islamic Azad University, Tehran, Iran. He received his MSc. and Ph.D. degrees in Mechanical Engineering from K. N. Toosi University of Technology in 2006 and 2013 respectively. His research interests include grasp planning of robotic systems and assistive robotics.

Ali Ghaffari was born in Neishaboor, Iran, in 1947. He received the B.S. degree from Sharif University of Technology, Tehran, Iran, the M.Sc. degree from the Georgia Institute of Technology, Atlanta, USA, and the Ph.D. degree from the University of California at Berkeley, CA, USA, all in mechanical engineering. He is currently a Professor in the Department of Mechanical Engineering, K. N. Toosi University of Technology, Tehran, Iran. His major research interests include nonlinear control, fuzzy logic control, dynamic systems, and robotics.